Chemical Engineering Journal 164 (2010) 155–167

Contents lists available at ScienceDirect

Chemical Engineering Journal

journal homepage: www.elsevier.com/locate/cej

A comparative study for simultaneous removal of urea, ammonia and carbon dioxide from industrial wastewater using a thermal hydrolyser

M.R. Rahimpour*, M.M. Barmaki, H.R. Mottaghi

Department of Chemical Engineering, School of Chemical and Petroleum Engineering, Shiraz University, Shiraz 71345, Iran

ARTICLE INFO

Article history:
Received 9 May 2010
Received in revised form 6 August 2010
Accepted 17 August 2010

Keywords:
Urea wastewater
Wastewater treatment
Urea thermal hydrolysis
Co-current mode
Counter-current mode

ABSTRACT

In this work a comprehensive study on wastewater treatment of industrial urea plants by thermal hydrolysis reactors is presented. A superior model is developed for two main co-current and counter-current modes of urea thermal hydrolysis reactor. In the proposed model the urea hydrolysis reactor is divided into several continuously stirred-tank reactors (CSTRs). The vapor–liquid equilibria are treated simultaneously with chemical reactions due to the complex features of urea hydrolysis system. The model provides temperature and concentration distributions of urea along the thermal hydrolyser. The validity of the proposed model was verified by the industrial observed data. Sensitivity analysis was carried out to investigate the effect of the various operating parameters on the performance of two types of hydrolysis reactors. Comparison of two kinds of hydrolysis reactors shows in order to observe the old environmental pollution standards, the co-current configuration of hydrolyser is more suitable than the counter-current one. However to achieve new environmental pollution standards and complete treatment, the counter-current configuration was the only acceptable practicable mode. Overall, this study results in valuable information about the performance of the co-current and counter-current modes of hydrolysis reactor in urea wastewater treatment.

1. Introduction

Urea is an organic compound with the chemical formula H_2NCONH_2 which is produced at industrial scale by the reaction between ammonia and carbon dioxide at high pressure and temperature [1]. This reaction produces one mole of H_2O for each mole of urea, equal to 300 kg of water for a ton of synthesized urea. Beside this synthetic water, the plant discharges all the water entering as steam for the final concentration of urea in vacuum sections. It can be estimated that the amount of discharged water from urea plant is 470–550 kg/ton of produced urea [2]. This liquid stream which contains ammonia, carbon dioxide and urea should be treated. Discharging this wastewater from the urea plant leads to the problem of water pollution as well as loss of urea and ammonia while ammonia presents significant danger to human health as a hazardous chemical and urea is considered deleterious in natural waterways that it promotes algae growth and hydrolyses slowly, releasing ammonia which is toxic to fish [3].

In the past decade, 100 ppm of urea was considered acceptable in discharge wastewater from urea plant, but currently, maximum acceptable concentration of urea is 10 ppm or should be less than 1 ppm in order to reuse for variety purposes such as cooling water or boiling feed water make-up [4,5]. Several processes have been suggested for treating the urea-containing streams due to current necessities for environmental protection and possibilities to upgrade this waste stream to a valuable high-pressure boiler feed water. Economically, it is preferred to remove and recover the urea and/or ammonia from the wastewater which includes ammonia and carbon dioxide desorption from the urea-wastewater, hydrolysing the urea in wastewater, total or partial desorption of the ammonia and carbon dioxide formed in the hydrolyser and condensation the off-gases in a reflux condenser [6].

In old urea plants, commercial thermal hydrolysis reactors are in operation at elevated temperature and pressure in co-current flow with steam, but in the best operating conditions even after very long residence times or high steam flow rate, it is not possible to achieve the urea and ammonia contents less than 20–25 ppm [7–9]. Recently, thermal hydrolysis reactors operate as a counter-current bubble column to improve the urea removal efficiency; the steam and feed streams flow counter-currently through the column. The bottom temperature of hydrolyser is maintained at about 180–230 °C while the top temperature is maintained at about 170–220 °C. In this manner, the ammonia and urea contents of the residual wastewater stream could be reduced to a level of 10 ppm or even less than 1 ppm, so this treated water could be used as boiler feed water or cooling water [10,11].

Rahimpour and Azarpour presented an equilibrium-based model regarding non-ideal solution for studying of the thermal

* Corresponding author. Tel.: +98 711 2303071; fax: +98 711 6287294.
E-mail address: rahimpor@shirazu.ac.ir (M.R. Rahimpour).

1385-8947/$ – see front matter © 2010 Elsevier B.V. All rights reserved.
doi:10.1016/j.cej.2010.08.046

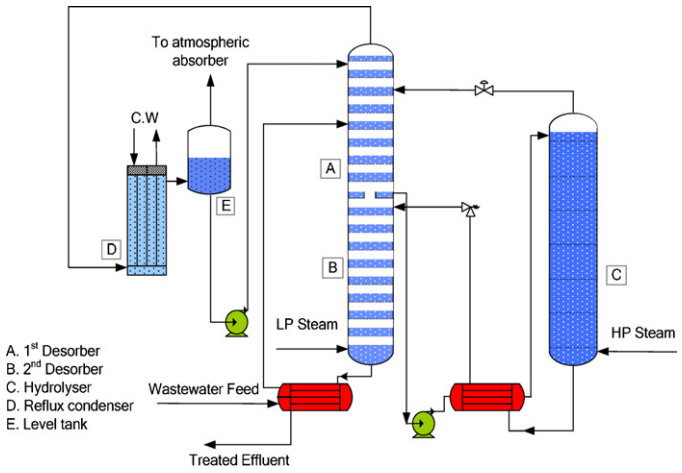

Fig. 1. New process for wastewater treatment.

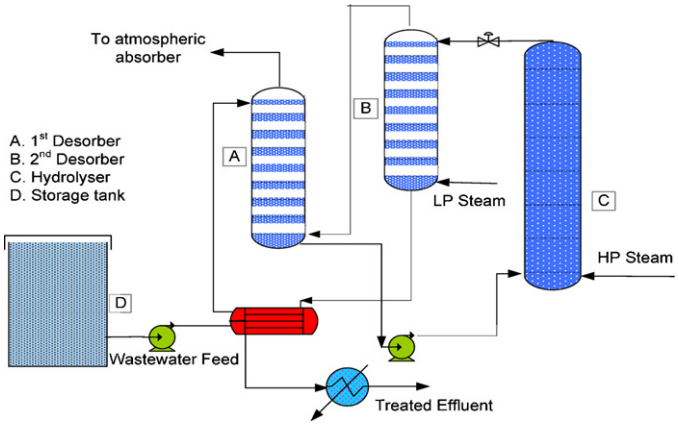

Fig. 2. Old process for wastewater treatment.

hydrolyser in co-current mode, but this model could not predict the reactor behavior with high accuracy [7]. Therefore, Rahimpour and Azarpour decided to investigate and simulate this urea thermal hydrolysis reactor as a multi-stage well-mixed model that combines with rate-based model and ideality of solution. This model showed the reactor behavior with better accuracy [12]. Also, Rahimpour proposed a non-ideal rate-based model for industrial urea thermal hydrolyser in co-current mode to incorporate the effect of liquid non-ideality on the urea thermal hydrolyser performance. The simulation results of this model showed good consistency with the plant data [8]. Moreover, Barmaki et al. studied an industrial counter-current hydrolyser for the first time that includes useful results [13]. After that, Rahimpour et al. investigated hydrolyser–desorber loop in order to removal of urea, ammonia and carbon dioxide [14].

Reviewing the literature reveals the information about urea removal from industrial wastewater by thermal hydrolysis reactor is very little detailed and patented, especially in the counter-current configuration [7,8,13]. Also, the co-current and counter-current modes of thermal hydrolysis reactor have not been compared yet and proposed model of the co-current hydrolyser in this work is different from previous models due to the consideration of two-phase stream along the hydrolyser. Furthermore, in previous work [8], only the forward reaction of hydrolysis reaction was considered while the new proposed model includes both of backward and forward reactions.

In this study, a general model for the reaction processes in a urea thermal hydrolyser using high-pressure steam has been developed. The combined effect of chemical reaction, liquid non-ideality and solution back mixing was treated by a multi-stage well-mixed model for the reactor and the objective of the current work is to compare the performance of thermal hydrolysis reactors in co-current and counter-current modes. Also, the effect of the key parameters on the urea, ammonia and carbon dioxide removal in both configurations of hydrolyser has been discussed.

2. Process description

Figs. 1 and 2 show the schematic diagrams of modern and conventional urea removal from wastewater of urea plant, respectively [6,15]. Both of them consist of a primary desorber column, which reduces the ammonia and carbon dioxide contents and operates at a low pressure. For the next column, the hydrolyser, it is important that the ammonia and carbon dioxide concentrations at the inlet are sufficiently low in order to maintain the system far from chemical equilibrium. Under these conditions the hydrolysis reactions proceed toward the ammonia and carbon dioxide production with reducing the urea content to virtually zero (less than 10 ppm). The residence time in the hydrolyser is approximately 1 h. The hydrolyser operates at relatively medium pressures (2 MPa) and temperature of about 200 °C. In the second desorber column which also operates at low pressure, the ammonia and carbon dioxide contents are decreased considerably. The stripping process is carried out in the second desorber by entrance of a low-pressure steam into the bottom of column. The vapors of the first desorber, which contain ammonia, carbon dioxide and water are condensed in a submerged reflux condenser and form a carbamate solution. Also, two process–process heat exchangers decrease the needed high-pressure and low-pressure steam consumption considerably.

Differences of modern and conventional wastewater treatment systems include:

- In the modern system, hydrolyser operates in the counter-current mode of operation (in counter of steam flow) and vapors from the hydrolyser are used for the stripping in the first desorber. Also, the height and diameter of this reactor are 16.5 and 2 m, respectively and has 13 sieve trays. However in the conventional system, hydrolyser operates in the co-current mode (in parallel of steam flow). In addition, the height and diameter of this reactor are 16 and 1.6 m, respectively and has 10 sieve trays.
- In the modern system, the first and second desorbers are integrated into one sieve tray column to save investment costs while in the conventional system two desorbers are separated.
- In the modern treatment system, temperature level of hydrolyser is more.

3. Reaction kinetics

The liquid phase contains physically dissolved and chemically combined components that are mainly present as ions and molecules, namely H_2NCONH_2 (1), H_2O (2), NH_4^+ (3), H_2NCOO^- (4), CO_2 (5) and NH_3 (6). The overall hydrolysis reaction of urea to ammonia and carbon dioxide is endothermic and proceeds rapidly above a temperature of approximately 130 °C according to the following simplified formula [1,16]:

$$NH_2CONH_2 + H_2O \Leftrightarrow 2NH_3 + CO_2 \quad (1)$$

The process of urea hydrolysis consists of two sequential steps. In the first step, ammonium carbamate is formed by the reaction between urea and water:

$$NH_2CONH_2(l) + H_2O(l) \Leftrightarrow H_2NCOO^- + NH_4^+$$
$$\Delta H_{298} = -23\,\text{kJ/mol} \quad (2)$$

In the next step, the ammonium and carbamate ions react to yield carbon dioxide and ammonia in liquid phase, while the vapor and liquid phases are at equilibrium:

$$H_2NCOO^- + NH_4^+ \Leftrightarrow 2NH_3(l) + CO_2(l)$$
$$\Delta H_{298} = 84\,kJ/mol \quad (3)$$

The completion of the reactions is favored by low pressure and high temperature. Besides improved reaction kinetics, the higher temperature improves the breakdown of the byproducts to ammonia and carbon dioxide. Reaction (2) is slow and exothermic, while reaction (3) is endothermic and fast in both directions, so it could be considered at equilibrium under the conditions found in the industrial hydrolyser [1,16]. Therefore reaction (2) is the rate controlling step and its rate is considered as the overall rate of urea hydrolysis. For chemical reactions in thermodynamically non-ideal systems, as shown elsewhere, the rate becomes [17–20]:

$$R^{ov} = k_f \left(a_1 a_2 - \frac{1}{K_2} a_3 a_4\right) = k_f \left[(\gamma_1 C_1)(\gamma_2 C_2) - \frac{1}{K_2}(\gamma_3 C_3)(\gamma_4 C_4)\right] \quad (4)$$

where k_f is the constant of forward reaction rate ($k_f = k_0 \exp(-E/RT)$) and K_2 is the equilibrium constant of reaction (2). The activity and activity coefficient of species i are a_i and γ_i, respectively. The molar concentration of species i is C_i. The experimental values of the pre-exponential factor and the activation energy in the Arrhenius expression of k_f are $k_0 = 10.417\,m^3/mol\,s$ and $E = 8.77803 \times 10^4$ J/mol, respectively [21].

The equilibrium constants for reactions (2) and (3) are defined as follows:

$$K_r(T) = K_{X,r}(X) K_{\gamma,r}(T, X) \quad r = 2, 3 \quad (5)$$

where the effects of liquid non-ideality on the reaction equilibria have been merged into a set of parameters, $K_{\gamma,r}(T, X)$ which are defined as:

$$K_{\gamma,r}(T, X) = \frac{\gamma_3(T, X)\gamma_4(T, X)}{\gamma_1(T, X)\gamma_2(T, X)} \quad r = 2 \quad (6)$$

$$K_{\gamma,r}(T, X) = \frac{\gamma_6^2(T, X)\gamma_5(T, X)}{\gamma_3(T, X)\gamma_4(T, X)} \quad r = 3 \quad (7)$$

and $K_{X,r}(X)$ is also defined as:

$$K_{X,r}(X) = \frac{x_3 x_4}{x_1 x_2} \quad r = 2 \quad (8)$$

$$K_{X,r}(X) = \frac{x_5 x_6^2}{x_3 x_4} \quad r = 3 \quad (9)$$

where X is the array of mole fractions in the liquid phase. Substituting Eqs. (6)–(9) into Eq. (7) results:

$$K_2(T) = \left(\frac{x_3 x_4}{x_1 x_2}\right)\left(\frac{\gamma_3(T, X)\gamma_4(T, X)}{\gamma_1(T, X)\gamma_2(T, X)}\right) x_2 \quad r = 2 \quad (10)$$

$$K_3(T) = \left(\frac{x_5 x_6^2}{x_3 x_4}\right)\left(\frac{\gamma_5(T, X)\gamma_6^2(T, X)}{\gamma_3(T, X)\gamma_4(T, X)}\right) \quad r = 3 \quad (11)$$

where the activity coefficient of each species in the reacting solution can be calculated from thermodynamic model. The following functional form:

$$\ln K_r(T) = \left(\frac{U_{1,r}}{T}\right) + U_{2,r} \ln T + U_{3,r} T + U_{4,r} \quad (12)$$

was adopted to describe the temperature dependence of the r reaction equilibrium constant [1,22]. In the above equation, U_r is a constant related to reaction of number r where tabulated in Table 1.

Table 1
Equilibrium constant parameters [22].

Function	Parameters			
	U_1	U_2	U_3	U_4
$\ln K_2$	−31,363	−64.26	−0.0595	482.11
$\ln K_3$	−11,046	−5.19	0.01115	51.47

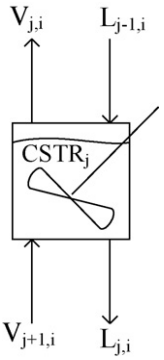

Fig. 3. Schematic diagram of the multi-stage well-mixed reactor model in counter-current mode.

4. Reactor model

In this section, the hypotheses and necessary equations to develop the steady state model of the urea hydrolysis reactor are described. In order to model of hydrolyser, the equilibrium (EQ) stage model is developed while the vapor and liquid phases are assumed to be in thermodynamic equilibrium.

The schematic illustrations of two types of equilibrium stages are presented in Figs. 3 and 4. In the counter-current mode, vapor from the below stage is brought into contact with the liquid from the above stage while in the co-current mode, vapor and liquid from below stage are brought into contact. According to type of hydrolysis reactor, the feed stream enters from the top or bottom of the hydrolyser and pure high-pressure steam stream enters from the bottom as the stripper. The hydrolyser is full of liquid and the movement of bubbles through the liquid phase causes mixing in the liquid phase. Moreover, there are several perforated plates at different levels inside the hydrolyser in order to prevent back mixing and further mixing between the two phases.

As noted above, for simulation purposes, the urea thermal hydrolyser can be approximated as a series of continuous multi-stage stirred-tank reactors (CSTRs), neglecting composition and temperature gradients within the stage contact volume. Rahimpour et al. considered the co-current and counter-current modes of urea thermal hydrolysis reactor as a sequence of continuously stirred-tank reactors (CSTRs) [8,12,13]. Throughout the following derivations, CSTRs in sequences will be referred to stages and num-

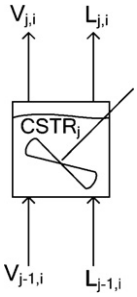

Fig. 4. Schematic diagram of the multi-stage well-mixed reactor model in co-current mode.

bered in direction of liquid flow. The stage (0) and stage (14) are hypothetical stages and indicate specifications of wastewater feed and inlet steam before entering to the hydrolyser. Overall, the goal of this assumption is facilitated deriving of material and energy balance equations for each CSTR.

4.1. Hypotheses

In this study, the developed mathematical model is based on the following assumptions:

(i) Hydrolysis reactions of take place only in the liquid phase.
(ii) The hydrolyser operates at steady state conditions.
(iii) Each stage is performs as mixed stirred-tank reactor (CSTR).
(iv) Each CSTR operates adiabatically.
(v) Phase equilibrium is achieved in each CSTR.
(vi) Vapor holdup is assumed to be negligible (hydrolyser is full of liquid).
(vii) The volatility of urea and ammonium carbamate is negligible.

4.2. Necessary equations

The rigorous developed mathematical model includes mass balance equation, heat balance equation, phase equilibrium equation, chemical equilibrium equation, summation equation and hydraulic equation.

4.2.1. Mass balance equations (M)

For counter-current configuration of hydrolysis reactor mass balance is expressed as:

$$M_{i,j} \equiv V_{j+1}y_{i,j+1} + L_{j-1}x_{i,j-1} + \alpha_{i,2}H_jR_j^{ov} + \alpha_{i,3}w - V_jy_j - L_jx_j = 0 \quad i = 1,\ldots,M \quad j = 1,\ldots,N \tag{13}$$

And for co-current configuration of hydrolysis reactor it is written as:

$$M_{i,j} \equiv V_{j+1}y_{i,j+1} + L_{j+1}x_{i,j+1} + \alpha_{i,2}H_jR_j^{ov} + \alpha_{i,3}w - V_jy_j - L_jx_j = 0 \quad i = 1,\ldots,M \quad j = 1,\ldots,N \tag{14}$$

where V_j and L_j are the vapor and liquid flow rates, respectively. x_{ij} and y_{ij} are the molar fraction in the liquid and vapor phases, respectively; and H_j is the volumetric liquid holdup (volume of each CSTR) and R_j^{ov} is the overall rate of reaction (2) on stage j which is obtained from Eq. (4). Also $\alpha_{i,r}$ is the stoichiometric coefficient of species i in reaction r (reactions (2) and (3)) which is positive for products and negative for reactants. The molar consumption rate of carbamate in reaction (3) is w. Approximately, the amounts of carbamate and ammonium ions are so little due to fast reaction (3), high value of equilibrium constant of reaction (3) and the imposed thermodynamic conditions.

4.2.2. Phase and chemical equilibrium equations (E)

Since the column is generally operated at the medium pressure, the vapor fugacity coefficients can be estimated with the PHS equation of Nakamura et al. [23]. For both configurations of hydrolysis reactors the basic phase equilibrium equation, as given by simplified Eq. (15):

$$E_{i,j} \equiv K_{i,j}x_{i,j} - y_{i,j} = 0 \quad i = 1,\ldots,M \quad j = 1,\ldots,N \tag{15}$$

Also Eq. (11) is expressed the same as MESH equations form in order to obtain the value of molar consumption rate of carbamate (w) in mass balance Eqs. (13) and (14) as follows:

$$E_{c,j} \equiv K_{3,j}(T) - \left(\frac{x_{5,j}x_{6,j}^2}{x_{3,j}x_{4,j}}\right)\left(\frac{\gamma_{5,j}(T,X)\gamma_{6,j}^2(T,X)}{\gamma_{3,j}(T,X)\gamma_{4,j}(T,X)}\right) = 0 \quad j = 1,\ldots,N \tag{16}$$

4.2.3. Summation equations (S)

$$S_j^x \equiv \sum_i^M x_{i,j} - 1 = 0 \quad j = 1,\ldots,N \tag{17}$$

$$S_j^y \equiv \sum_i^M y_{i,j} - 1 = 0 \quad j = 1,\ldots,N \tag{18}$$

4.2.4. Heat balance equation (H)

Considering that heat effect of reaction is different for the components enthalpies, the enthalpy of formation is employed. For counter-current configuration of hydrolysis reactor, the heat balance equation related to jth tray can be written as:

$$H_j \equiv \sum_i^M V_{i,j+1}H_{i,j+1}^v + \sum_i^M L_{i,j-1}H_{i,j-1}^l - \sum_i^M V_{i,j}H_{i,j}^v - \sum_i^M L_{i,j}H_{i,j}^l = 0 \quad j = 1,\ldots,N \tag{19}$$

And for co-current configuration, it is written as:

$$H_j \equiv \sum_i^M V_{i,j+1}H_{i,j+1}^v + \sum_i^M L_{i,j+1}H_{i,j+1}^l - \sum_i^M V_{i,j}H_{i,j}^v - \sum_i^M L_{i,j}H_{i,j}^l = 0 \quad j = 1,\ldots,N \tag{20}$$

where $H_{i,j}^v$ and $H_{i,j}^l$ are the enthalpies of vapor and liquid components on the stage j, respectively.

4.2.5. Hydraulic equations (P)

There is approximately 0.2 MPa pressure drop along the both of hydrolysis reactors. The pressure drop over sieve tray may be estimated using proper correlations, so the pressure drop is expressed for counter-current configuration of hydrolysis reactor as follows:

$$P_1 \equiv p_{top} - p_1 = 0 \quad j = 1 \tag{21}$$

$$P_j \equiv p_j - \Delta p_{j-1} - p_{j-1} = 0 \quad j = 2,\ldots,N \tag{22}$$

and for co-current one, it is written as:

$$P_1 \equiv p_{bottom} - p_1 = 0 \quad j = 1 \tag{23}$$

$$P_j \equiv p_j + \Delta p_{j-1} - p_{j-1} = 0 \quad j = 2,\ldots,N \tag{24}$$

where p_{top} is the specified pressure of the tray at the top of the counter-current hydrolyser and p_{bottom} is the specified pressure of the tray in the bottom of the co-current hydrolyser. Also Δp_{j-1} is the pressure drop per tray from stage $j-1$ to stage j.

5. Numerical solution

The basic structure of the model is consisted of nonlinear algebraic equations of mass and energy conservative rules of both the vapor and liquid phases, which have to be coupled with equations of

Table 2
Input specifications of the industrial co-current urea thermal hydrolyser [15].

Feed specifications	Case 1		Case 2	
	Liquid phase input	Vapor phase input	Liquid phase input	Vapor phase input
Temperature (°C)	138	380	138	380
Pressure (kg/cm^2)	18.3	25	18.3	25
Component molar rate (kmol/h)				
Water	1988.33	177.78	1988.33	144.45
Urea	7.08	0	7.08	0
CO_2	0.42	0	0.42	0
NH_3	1.08	0	1.08	0
Total (kmol/h)	1996.91	177.78	1996.91	144.45

the kinetic model and auxiliary correlations. These set of nonlinear equations must be solved by iterative techniques.

A wide variety of iterative solution procedures for solving nonlinear algebraic equations has appeared in the literature. In general, these procedures make use of equation partitioning in conjunction with equation tearing and/or linearization by Newton–Raphson techniques, which are described in detail by Myers and Seider [24]. For intermediate cases, the equation-tearing technique may fail to converge; in that case, the either a Newton–Raphson method or a combined tearing and Newton–Raphson technique is necessary [25]. More general capable procedures of solving all types of multi-component, multi-stage separation problems are based on the solution of all the MESH equations, or combinations thereof, by simultaneous correction (SC) techniques, often using the Newton–Raphson method. For proper use, the Newton–Raphson method demands the evaluation of the partial derivatives of all the equations with respect to all the variables. However, the partial derivatives of thermodynamic properties with respect to temperature and composition are often awkward to obtain and this makes the Newton–Raphson method difficult to use. To improve accuracy and speed up the computation, all of the derivatives of thermodynamic properties in this study are obtained analytically. The resulting Jacobian matrix has a block tridiagonal structure. Linear systems with a block tridiagonal coefficient matrix can be solved quite efficiently using the Thomas algorithm [26].

Let

$$(F(X)) = 0 \tag{25}$$

where

$$X = [X_1, X_2, \ldots, X_j, \ldots, X_N]^{\mathrm{T}} \tag{26}$$

and

$$F = [F_1, F_2, \ldots, F_j, \ldots, F_N]^{\mathrm{T}} \tag{27}$$

where X_j is the vector of unknown variables for stage j and F_j is the vector of model equations for stage j arranged in the order

$$X_j = [T_j, x_{1,j}, x_{2,j}, \ldots, x_{i,j}, \ldots, x_{M,j}, y_{1,j}, y_{2,j}, \ldots, y_{i,j}, \ldots, y_{M,j}, L_j, V_j, p_j, w]^{\mathrm{T}} \tag{28}$$

$$F_j = [H_j, M_{1,j}, M_{2,j}, \ldots, M_{i,j}, \ldots, M_{M,j}, E_{1,j}, E_{2,j}, \ldots, E_{i,j}, \ldots, E_{M,j}, S_j^x, S_j^y, P_j, E_{c,j}]^{\mathrm{T}} \tag{29}$$

The Newton–Raphson iteration is performed by solving the corrections ΔX to the output variables, which in matrix form becomes:

$$\Delta X^k = -\left[\left(\frac{\partial F_i}{\partial X_i}\right)^{-1}\right]^k F^K \tag{30}$$

where k stands for the iteration number. These corrections are used to compute the next approximation to the set of output variables from:

$$X^{k+1} = X^k + t\Delta X^k \tag{31}$$

Table 3
Input specifications of the industrial counter-current urea thermal hydrolyser [6].

Feed specifications	Liquid phase input	Vapor phase input
Temperature (°C)	197	308
Pressure (kg/cm^2)	18.3	20.3
Component molar rate (kmol/h)		
Water	2037.5	86.9
Urea	9	0
CO_2	1.3	0
NH_3	19.6	0
Total (kmol/h)	2067.4	86.9

where t is scalar step factor or relaxation factor. The quantity $(\partial F/\partial X)$ is the Jacobian or $(N \times N)$ matrix of blocks of partial derivatives of all the functions with respect to all the output variables. A scalar stepping factor (t) was used in order to ensure convergence. When t was optimized to a value between 0 and 1 during every iteration, convergence was achieved to yield a feasible solution.

6. Model validation

The validation of steady state model was carried out by comparison of the model results with the plant data. The input data of the co-current and counter-current modes of hydrolysis reactor have been summarized in Tables 2 and 3, respectively.

The model results and the corresponding observed data of the industrial co-current and counter-current thermal hydrolysis reactors of urea plants have been presented in Tables 4 and 5. It was observed that, the steady state model performed satisfactorily well at the industrial conditions and a good agreement was obtain between the plant data and the simulation data.

7. Results and discussion

In this section, the results of the simulation of two types of hydrolysis reactors (co-current and counter-current modes) are compared with each other in terms of the temperature and the flow rates of urea versus length of reactor. Also, the sensitivity analysis is carried out to investigate the effect of operating parameters on the reactor performance. Firstly, two hydrolysis reactors (the industrial counter-current hydrolyser and hypothetical co-current one) are compared with each other at the same conditions as mentioned in Table 3. The all specifications of the co-current mode are similar with the counter-current one, except that in the co-current mode the steam is flowed in the same direction with entering wastewater stream. The stages are numbered from the bottom to the top of reactor for the co-current configuration and numbered from the top to the bottom for the counter-current configuration.

As liquid moves along the hydrolyser, temperature undergoes variations. The comparison between temperature profiles along

Table 4
Comparison of calculated results with the observed plant data for co-current hydrolyser under the design specifications and input data [15].

	Case 1 (3.2 ton/h steam)			Case 2 (2.6 ton/h steam)		
	Observed	Model	Error (%)	Observed	Model	Error (%)
Temperature (°C)	195	195.6	+0.3	185	185.5	+0.27
Component molar rate (kmol/h)						
Water	2159.1	2159.11	≅0.0	2125.91	2125.92	≅0.0
Urea	0.071	0.077	+8.4	0.212	0.222	+4.7
CO_2	7.43	7.42	−0.13	7.29	7.28	−0.13
NH_3	15.11	15.09	−0.06	14.83	14.81	−0.07
Total (kmol/h)	2181.71	2181.70	≅0.0	2148.24	2148.23	≅0.0

Table 5
Comparison of calculated results with the observed plant data for counter-current hydrolyser under the design specifications and input data [6].

	Liquid phase output			Vapor phase output		
	Observed	Model	Error (%)	Observed	Model	Error (%)
Temperature (°C)	207	207.6	+0.3	194.2	193.3	0.5
Component molar rate (kmol/h)						
Water	2066.7	2070.5	+0.2	48.15	44.37	−7.8
Urea	<10 ppm	7 ppm	–	0	0	–
CO_2	0.15	0.14	−6.7	10.18	10.16	−0.2
NH_3	33.63	33.33	−0.9	3.91	4.19	+7.1
Total (kmol/h)	2100.48	2103.97	+0.2	62.24	58.72	−5.6

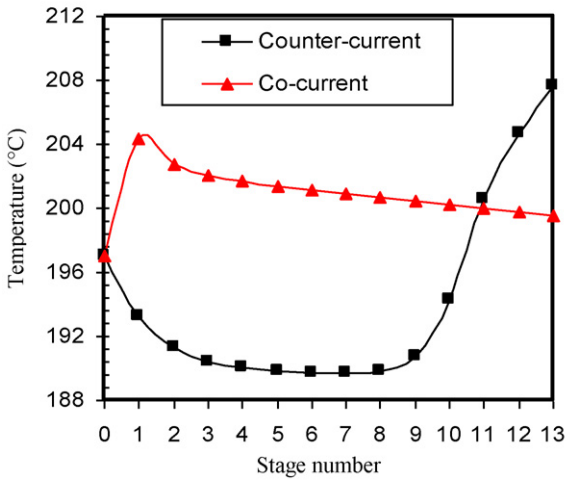

Fig. 5. Temperature profile of reacting material along the both types of hydrolysis reactors where the operating conditions are same as Table 3.

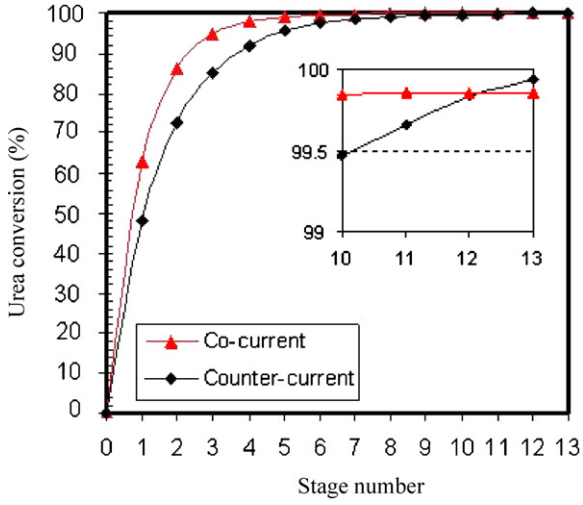

Fig. 6. Conversion of urea along the both types of hydrolysis reactors.

both types of hydrolysis reactors have been presented in Fig. 5. It can be seen that temperature profile of co-current hydrolyser suddenly increases due to the injection of high-pressure steam and then decreases along the reactor due to the endothermic overall reactions while temperature profile of counter-current mode has two parts in this figure. At the first segments of the hydrolyser, the temperature of reacting material decreases owing to the endothermic overall reactions, then increases because of injection of high-pressure steam. This figure indicates at the end, the temperature of the counter-current hydrolyser is higher than the co-current one because of steam injection. Also, temperature variation along the two types of hydrolyser is not much. The possible explanation for this behavior is that the weight percent of water is so much larger than other components, and then the heat of reactions has no significant effect on the stream temperature.

Figs. 6 and 7 show the conversion and concentration of urea along the two types of hydrolysis reactors. As demonstrated in these figures, at the first segments of co-current hydrolyser the urea conversion is higher (urea mole flow rate is less) than counter-current one, but at the end the urea conversion of the counter-current hydrolyser is higher (urea molar flow rate is less) than the co-current one. It should be noted that the outlet urea content of the counter-current hydrolyser is virtual zero due to complete hydrolysis reactions and the conversion is approximately 99.95%. Also, the urea conversion and urea molar flow rate profiles of the co-current hydrolyser have horizontal asymptotes that indicate considerable decrease of urea removal efficiency at the end of hydrolyser.

7.1. *Effect of inlet temperature of wastewater*

Inlet temperature of wastewater has an influence on the urea removal performance as demonstrated in Fig. 8. This figure indicates the increase of the inlet temperature of wastewater improves

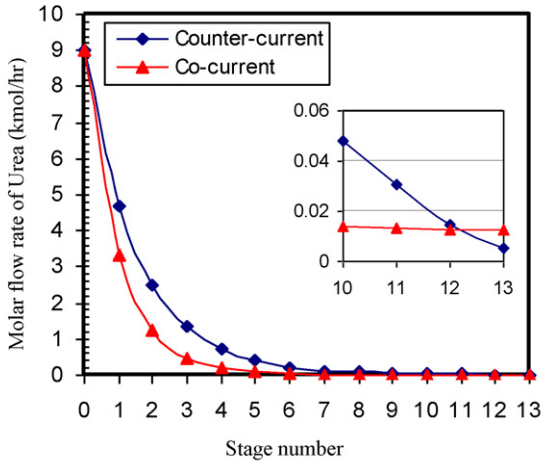

Fig. 7. Molar flow rates of urea along the both types of hydrolysis reactors.

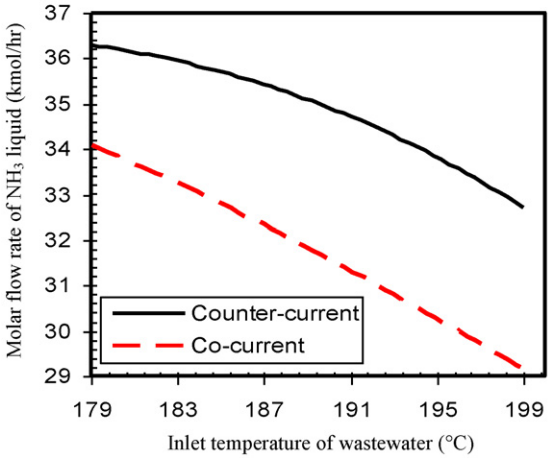

Fig. 9. Molar flow rates of ammonia in liquid phase of ammonia versus inlet temperature of wastewater in the both types of hydrolysis reactors where the other operating conditions are the same as Table 3.

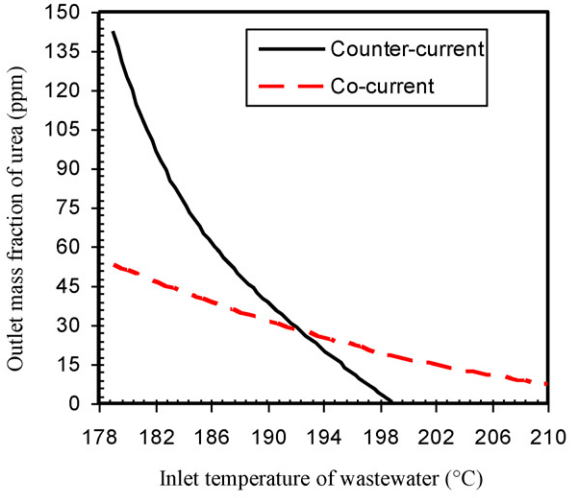

Fig. 8. Outlet mass fraction of urea versus inlet temperature of wastewater in the both types of hydrolysis reactors where the other operating conditions are the same as Table 3.

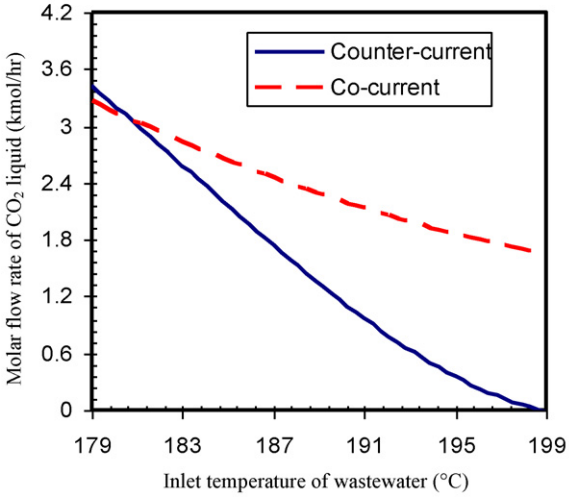

Fig. 10. Molar flow rates of carbon dioxide in liquid phase versus inlet temperature of wastewater in the both types of hydrolysis reactors where the other operating conditions are the same as Table 3.

the urea removal performance due to endothermic overall reactions. Also as can be seen at the temperature of 193 °C, two hydrolysis reactors have the same efficiency, but higher than this temperature, the efficiency of counter-current hydrolyser is more than co-current one and consequently the urea content in the outlet liquid is less. As shown in this figure, in the counter-current case, by increase of inlet wastewater temperature, the urea content rapidly goes to zero virtually. However, in the co-current case, the urea content profile goes to a horizontal asymptote. Therefore, large change in the inlet wastewater temperature is required to obtain a small decrease in the outlet urea concentration due to the apparent first order reaction of urea hydrolysis. This figure shows in order to achieve new environmental standards such as 1 ppm of urea content in outlet liquid stream, only the counter-current configuration is appropriate.

If the inlet temperature of wastewater increases, molar flow rates of the ammonia and carbon dioxide decrease in the outlet liquid stream because of higher temperature profile along hydrolyser which shifts the vapor–liquid equilibrium to the vapor phase. As can be seen from Fig. 9, when temperature increases from 179 to 199 °C, the ammonia content decreases slightly owing to the imposed medium pressure in the both of hydrolysis reactors. Therefore, it is not possible to decrease the ammonia in the outlet liquid stream in order to reach less than 10 ppm only by increase of the inlet temperature of wastewater. Moreover as shown in Fig. 10, by increase of the inlet wastewater, the carbon dioxide content in the outlet liquid stream of the counter-current hydrolyser become less than the co-current one and lastly decreases into virtual zero, while in the co-current case, the carbon dioxide profile has a horizontal asymptote. In addition, as clearly demonstrated in these figures an increase in the inlet temperature would result in a higher purity of water, due to the increasing extent of reactions at higher temperature and shift of the vapor–liquid equilibria to the vapor phase.

7.2. Effect of inlet flow rate of wastewater

The role of wastewater flow rate in urea removal at identical operating conditions is shown in Fig. 11. From this figure, lower wastewater flow rate provides less urea concentration than higher flow rate. Also, the comparison between outlet urea profiles shows

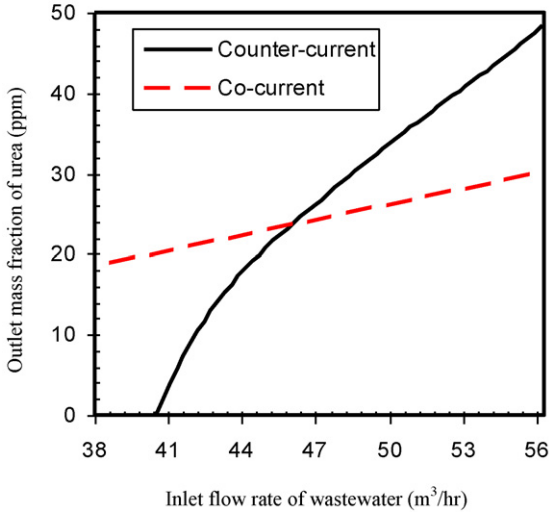

Fig. 11. Outlet mass fraction of urea versus inlet flow rate of wastewater in the both types of hydrolysis reactors where the other operating conditions are the same as Table 3.

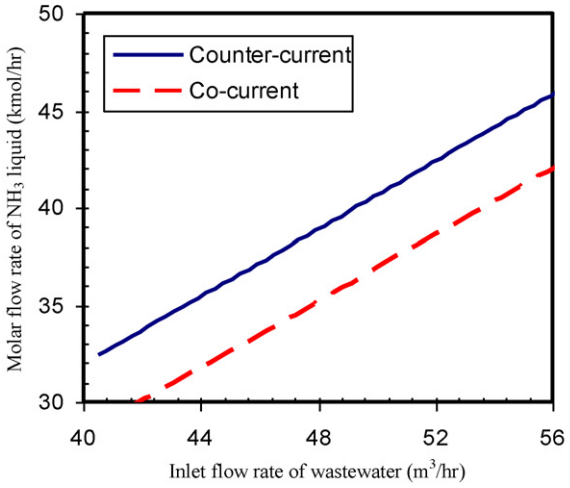

Fig. 12. Molar flow rates of ammonia in liquid phase versus inlet flow rate of wastewater in the both types of hydrolysis reactors where the other operating conditions are the same as Table 3.

in counter-current case by decrease of wastewater flow rate less than 46 m^3/h, the outlet urea content decrease sharply into virtual zero. However, in co-current case urea conversion decreases slightly and achieving to less than 5 ppm of urea content is impractical. From the new environmental standards point of view, the comparison shows preference of the counter-current hydrolyser over the co-current one. Moreover, as can be seen, if flow rate of wastewater increases more than 46 m^3/h, efficiency of the co-current hydrolyser becomes higher than the counter-current one. The increase in the wastewater flow rate causes a decrease in the residence time of reactants and lower profile of temperature along the hydrolyser, so the urea conversion decreases. Also, Figs. 12 and 13 show the concentrations of ammonia and carbon dioxide in the outlet liquid of hydrolysis reactors as a function of the inlet flow rate of wastewater. It can be seen, by increase of inlet flow rate of wastewater, the ammonia and carbon dioxide contents increase linearly.

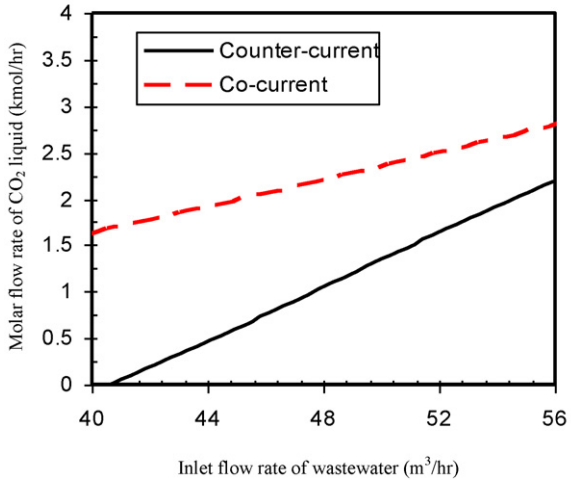

Fig. 13. Molar flow rates of carbon dioxide in liquid phase versus inlet flow rate of wastewater in the both types of hydrolysis reactors where the other operating conditions are the same as Table 3.

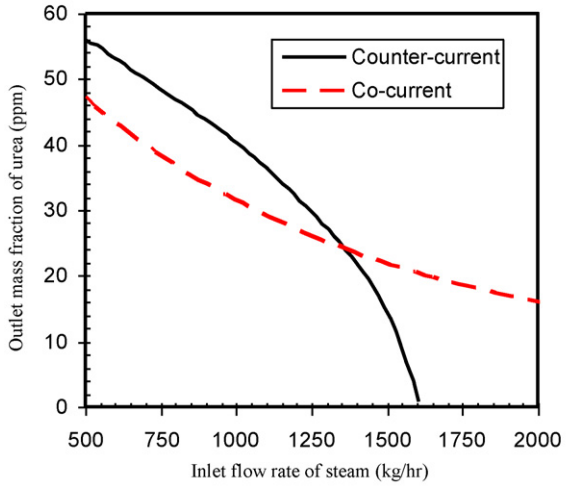

Fig. 14. Outlet mass fraction of urea versus inlet flow rate of steam in the both types of hydrolysis reactors where the other operating conditions are the same as Table 3.

7.3. *Effect of steam flow rate*

The role of steam mass flow rate in urea removal at a specified inlet wastewater temperature is shown in Fig. 14. As can be seen from this figure, higher steam mass flow rate maintains a higher temperature level in the hydrolyser which would change the liquid temperature profile and extends of hydrolysis reactions and consequently enhances the urea removal. Furthermore, the comparison of two outlet urea profiles of co-current and counter-current hydrolysis reactors demonstrates to satisfy the new environmental pollution standards, the co-current hydrolyser is not suitable and it cannot reduce urea content less than 10 ppm even if the steam flow rate increases so much. In fact, by increase of the steam flow rate, the outlet urea content of the counter-current hydrolyser decreases quickly and the slope of its profile becomes sharp while in the co-current one, it approaches the horizontal asymptote. The difference of these profiles is related to the lower temperature at the end of the co-current hydrolyser. In addition, a change in the flow rate of the entering steam has an effect on the concentrations of ammonia and carbon dioxide in the outlet liquid stream. As it is clearly demonstrated in Fig. 15, an increase

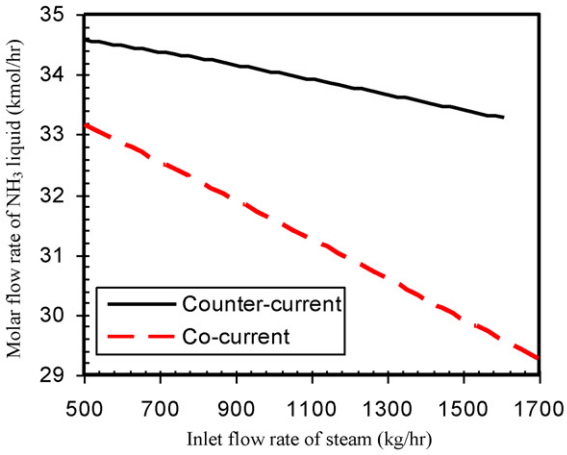

Fig. 15. Molar flow rates of ammonia in liquid phase of ammonia versus inlet flow rate of steam in the both types of hydrolysis reactors where the other operating conditions are the same as Table 3.

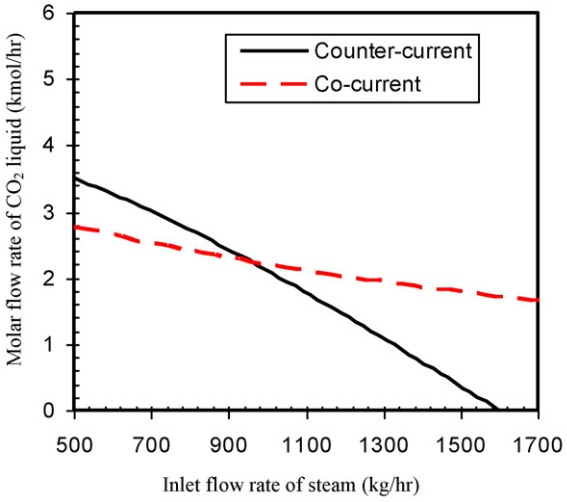

Fig. 16. Molar flow rates of carbon dioxide in liquid phase versus inlet flow rate of steam in the both types of hydrolysis reactors where the other operating conditions are the same as Table 3.

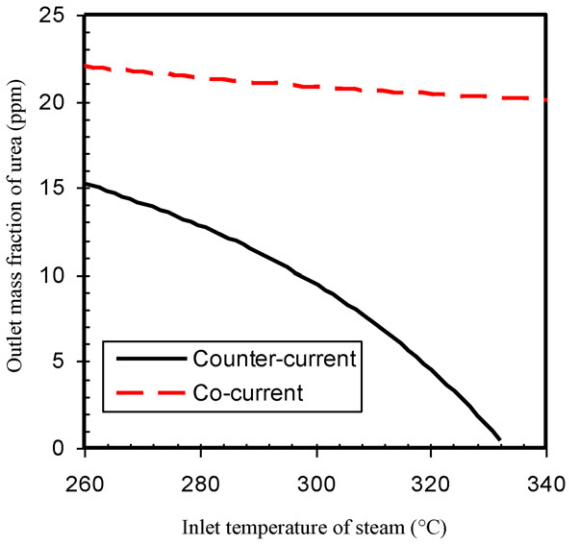

Fig. 17. Outlet mass fraction of urea versus inlet temperature of steam in the both types of hydrolysis reactors where the other operating conditions are the same as Table 3.

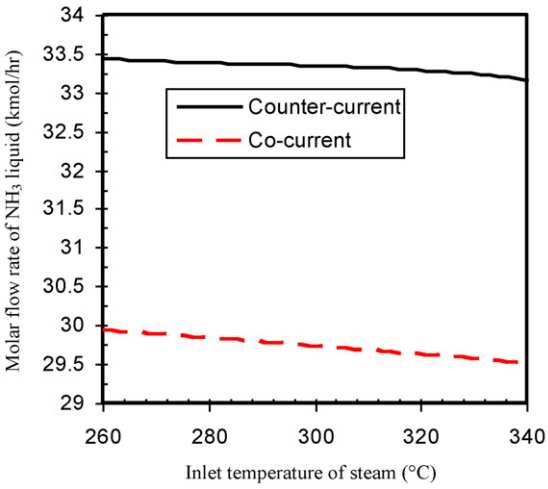

Fig. 18. Molar flow rates of ammonia in liquid phase versus inlet temperature of steam in the both types of hydrolysis reactors where the other operating conditions are the same as Table 3.

in the stream flow rate would result in a lower concentration of ammonia in the exit liquid. This figure shows the outlet ammonia content of the co-current hydrolyser is always less than the counter-current one. Also, Fig. 16 shows the outlet carbon dioxide content of the counter-current hydrolyser decreases to so little value, if the steam flow rate increases. As can be seen, the outlet carbon dioxide content of the co-current hydrolyser cannot change so much with respect to increase of the steam flow rate. The reason for decrease of the ammonia and carbon dioxide contents in the outlet liquid is due to temperature increasing in hydrolysis reactors.

7.4. Effect of inlet temperature of steam

Fig. 17 shows effect of temperature of steam on the urea concentration in the outlet liquid stream of two types of hydrolysis reactors. It is clear that increase of temperature affects counter-current hydrolyser performance more than co-current one. From this figure, decrease of outlet urea content of co-current hydrolyser with respect to increase of steam temperature is low, so reduction of the urea content in outlet liquid in order to achieve less than 10 ppm is not practical. However in the counter-current mode, it decreases easily so that satisfies the new environmental pollution. Temperature increasing of steam improves urea removal in two paths. Firstly, causes higher temperature profile along the hydrolyser and consequently increases the rate of hydrolysis reactions toward the urea removal. Secondly, decreases the ammonia and carbon dioxide contents which are produced in the liquid phase along the hydrolyser according to the vapor–liquid equilibrium, so the second reaction of hydrolysis reactions shifts to right and extents the hydrolysis reactions. Figs. 18 and 19 demonstrate effect of increase of steam temperature on the ammonia and carbon dioxide contents in the outlet liquid stream. It is clear that changes of the ammonia and carbon dioxide values are small with respect to increase of steam temperature.

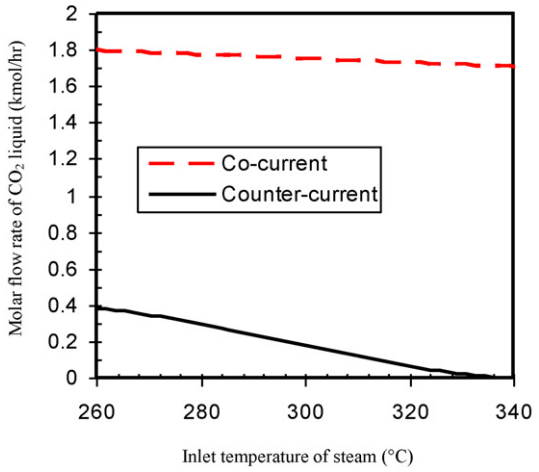

Fig. 19. Molar flow rates of carbon dioxide in liquid phase versus inlet temperature of steam in the both types of hydrolysis reactors where the other operating conditions are the same as Table 3.

7.5. Investigation of hydrolysis reactor configuration change from co-current to counter-current in conventional urea plant

As can be seen from comparison between co-current and counter-current modes of hydrolyser, results show under particular conditions, efficiency of the counter-current hydrolyser is higher and to observe the new environmental standards application of the counter-current hydrolyser is essential. The results from the comparison between the outlet urea content profiles as shown in Figs. 8, 11, 14 and 17, confirm the profiles of outlet urea content in the co-current hydrolyser have horizontal asymptotes that illustrate decrease of urea less than 10 ppm is so difficult while the urea content could be decreased even 1 ppm in the counter-current hydrolyser. The main reason of this difference is the presence of chemical equilibria that form at the end of reactor. In the counter-current mode, these chemical equilibria are shifted to enhance urea hydrolysis more than the co-current mode because of higher temperature at the end of the hydrolyser. Now, with respect to preference of the counter-current hydrolyser, a questionable point raises that would urea removal from wastewater of conventional urea plants improve, if configuration of hydrolyser changes from co-current to counter-current under the same operating conditions corresponds to Table 4 case 1?

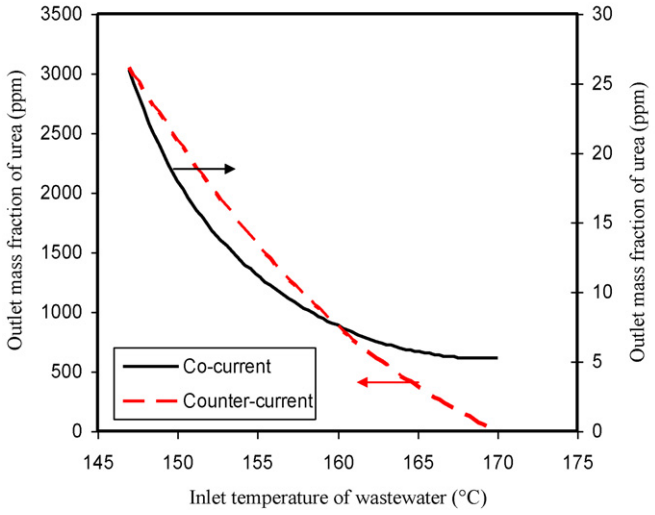

Fig. 20. Outlet mass fraction of urea versus inlet temperature of wastewater in the both types of hydrolysis reactors where the other operating conditions are the same as Table 2 case 1.

Fig. 20 shows the outlet urea content of two types of hydrolysis reactors as a function of inlet temperature of wastewater. As can be seen, the outlet urea content increases more than 3000 ppm when configuration of industrial co-current hydrolyser changes to hypothetical counter-current mode. However, if the inlet temperature of wastewater increases up to 170 °C, the outlet urea content of hypothetical counter-current hydrolyser rapidly decreases less than few ppm even less than 1 ppm while industrial co-current one cannot decrease less than 5 ppm even if wastewater warm up to 190 °C. Due to difficulty of warm up inlet wastewater to higher temperatures and necessity of considerable modification in conventional urea plant in order to change the co-current mode of hydrolyser to the counter-current one, it is better and practical to install additional hydrolyser and desorber at the end of process to keep current operating conditions and satisfy the new environmental pollution standards.

8. Conclusions

One of the most effective ways to remove urea from industrial wastewater is hydrolysing it in the thermal hydrolysis reactor and desorbing the ammonia and carbon dioxide which is formed. In this study, the hydrolysis of urea was mechanistically modeled in the industrial scale. Two types of industrial thermal hydrolysis reactors as co-current and counter-current configurations were considered. In order to develop the model, hydrodynamic and reaction sub-models were coupled with each other in the modeling of the hydrolyser. The hydrodynamic of the urea thermal hydrolyser was simulated by a sequence of CSTRs in series. The profiles of the urea concentration and temperature along two reactors have been compared. This comparison shows conversion and temperature of outlet treated liquid of the counter-current hydrolyser were more than the co-current one. Also, this comparison shows if we are looking for old environmental pollution standards (less than 100 ppm for urea effluent), the co-current configuration of hydrolyser is more suitable than the counter-current one. However, in order to observe the new environmental pollution standards (less than 10 ppm or even 1 ppm for urea effluent) the counter-current configuration was the only acceptable practicable mode. Moreover, the results of models were compared with real plant data at various conditions of conventional and modern hydrolysis reactors. In both cases, good consistency was observed between the plant data and the results of the model. Also, the effects of key operating parameters such as the inlet temperature and flow rate of wastewater and steam on the performance of two types of the hydrolysis reactors were investigated. The proposed models are useful for a better control of the currently operating units and design of new hydrolyser in wastewater treatment section of urea plants.

Acknowledgments

The authors would like to thank Khorasan Petrochemical Company and Shiraz Petrochemical Complex for providing valuable process and technical data. Also the authors would like to appreciate financial support by the Shiraz Petrochemical Complex.

Appendix A. Thermodynamics

A rigorous thermodynamic model is critical for process simulation. In urea wastewater treatment, it is involved a system under pressure ranging from 1.7 to 4.5 MPa and temperature from 180 to 220 °C depending on different techniques. The chemical reac-

tions take place in the liquid phase and the vapor–liquid equilibria of volatile components should be considered simultaneously [27]. There are several thermodynamic models to describe the non-ideality of NH_3–CO_2–H_2O–urea system [1,28–31]. Edwards's model is applicable to dilute weak electrolyte systems [29]; Sander's model [32–34] and Isla's model [1] could yield better results within HP region. In this study, the thermodynamic framework to describe liquid activity coefficients of molecular and ionic species in NH_3–CO_2–H_2O–urea system is based on the model developed by Isla et al. The volatility of urea and ammonium carbamate is negligible and ions could not leave from the liquid phase to the vapor phase, so there are only three molecular components including H_2O, NH_3, and CO_2 in the vapor phase. The vapor–liquid equilibria can be expressed with the following relationships:

$$NH_3(l) \Leftrightarrow NH_3(g) \quad (A.1)$$

$$CO_2(l) \Leftrightarrow CO_2(g) \quad (A.2)$$

$$H_2O(l) \Leftrightarrow H_2O(g) \quad (A.3)$$

As follows in Table A.1, the extended UNIQUAC equation consists of three items [1,32–34]. The volume and surface factors, r_i and q_i, are tabulated in Table A.2. All of the binary interaction parameters are listed in Table A.3.

At phase equilibrium, the following relationship must be satisfied for water and ammonia:

$$x_i\gamma_i f_i^0 \exp\left(\frac{v_i^l P}{RT}\right) = Py_i\Phi_i \quad (A.4)$$

where f_i^0 is defined as the standard fugacity at the system temperature and zero pressure.

For carbon dioxide, Henry's law is applicable, and vapor–liquid equilibrium equation is represented as Eq. (A.5), while H_{CO_2} is the Henry's constant of carbon dioxide:

$$x_i\gamma_i H_{CO_2} \exp\left(\frac{v_i^l(P-P_2^s)}{RT}\right) = Py_i\Phi_i \quad (A.5)$$

vapor fugacity coefficient Φ_i was estimated with the PHS equation of Nakamura et al. [23].

The temperature dependence of the reference fugacity of pure liquid ammonia at zero pressure and Henry's constant for carbon dioxide are modeled as:

$$\ln f_{NH_3}^0(T) = \frac{A_1}{T} + A_2\ln T + A_3T + A_4 \quad (A.6)$$

$$\ln H_{CO_2}(T) = \frac{B_1}{T} + B_2\ln T + B_3T + B_4 - q_5\tau_{5,2} \quad (A.7)$$

where q_5 and $\tau_{5,2}$ are obtained from Table A.1. All parameters of ammonia fugacity and carbon dioxide Henry's constant are represented in Table A.4.

Table A.1
Parameters of extended UNIQUAC model [1].

Parameter	Expression
$\gamma_i(T,x)$	$\ln\gamma_i(T,x) = \ln\gamma_i^C(X) + \ln\gamma_i^{RE}(T,X) + \ln\gamma_i^{DH}(X,T)$
$\gamma_i^C(X)$	$\ln\gamma_i^C(X) = \ln\left(\frac{\Phi_i}{X_i}\right) + \frac{Z}{2}q_i\ln\frac{\bar{v}_i}{\Phi_i} + l_i - \frac{\Phi_i}{X_i}\sum_j X_j l_j$
$\gamma_i^{RE}(T,X)$	$\ln\gamma_i^{RE}(T,X) = q_i\left[1 - \ln\left(\sum_{j=1}^{m}\bar{v}_j\tau_{ji}\right) - \sum_{j=1}^{m}\frac{\bar{v}_j\tau_{ij}}{\sum_{k=1}^{m}\bar{v}_k\tau_{kj}}\right]$
$\bar{v}_i$	$\bar{v}_i = \frac{q_iX_i}{\sum_j q_jX_j}$
Φ_i	$\Phi_i = \frac{\bar{r}_iX_i}{\sum_j \bar{r}_jX_j}$
l_i	$l_i = \frac{Z}{2}(\bar{r}_i - q_i) - (\bar{r}_i - 1)$
τ_{ij}	$\tau_{ij} = \exp\left(\frac{-a_{ij}}{T}\right), \quad a_{ii} = a_{jj} = 0$
$\gamma_i^{DH}(T,X)$	$\ln\gamma_i^{DH}(T,X) = \left(\frac{2A}{b^3}\right)M_i\left[1 + bI^{1/2} - \frac{1}{1+bI^{1/2}} - 2\ln(1+bI^{1/2})\right]$
$\gamma_i^{DH}(T,X)$	$\ln\gamma_i^{DH}(T,X) = -z_i^2\frac{AI^{1/2}}{1+BI^{1/2}}$
I	$I = \left(\frac{1}{2}\right)\sum m_jz_j^2$
Z	$Z = 35.2 - 0.1272T + 0.00014T^2$

Table A.2
Pure component parameters of extended UNIQUAC model [1].

Component	i	q_i	r_i	Units
H_2NCONH_2	1	2.00	2.16	–
H_2O	2	1.40	0.92	–
NH_4^+	3	0.99	0.91	–
H_2NCOO^-	4	1.58	1.71	–
CO_2	5	1.12	1.32	–
NH_3	6	1.00	1.00	–

Table A.3
Binary interaction parameters of extended UNIQUAC model [1].

i	j					
	1	2	3	4	5	6
1	0.0	91.7	−162.2	−166.2	269.0	−532.5
2	−110.0	0.0	355.6	0.9	−401.5	−626.3
3	272.8	−272.8	0.0	1476.5	−653.6	−12.4
4	221.6	−96.6	−337.2	0.0	−302.6	−62.3
5	670.5	2623.7	836.1	−204.8	0.0	−610.0
6	357.1	847.3	−190.7	335.0	−291.4	0.0

Table A.4
Ammonia fugacity and carbon dioxide Henry's constant parameters.

Function	Parameters			
	$10^{-2}A_1$	10^2A_2	10^4A_3	$10A_4$
$\ln f_{NH_3}^0$	−25.141	28.417	−25.759	146.46
Function	Parameters			
	$10^{-2}B_1$	10^2B_2	10^3B_3	$10B_4$
$\ln H_{CO_2}$	−26.56	−35.05	63.216	181.575

Appendix B. Equation of state

The chemical literature is rich in articles describing equations of state for simple non-polar gases but little attention has been given to an equation of state that is also applicable to polar gases. In this work because of existence of gaseous mixture containing highly polar molecules (ammonia, water) and non-polar molecule (carbon dioxide), the semi-empirical equation of state is proposed which provides accurate estimates of thermodynamic properties for this gas mixture [28]. The simple perturbed-hard-sphere equation is given by Nakamura et al. as follows:

$$P = \frac{RT}{v}\left[\frac{1+\xi+\xi^2-\xi^3}{(1-\xi)^3}\right] - \frac{a}{v(v+c)} \quad (B.1)$$

where P is the pressure, v is the molar volume, T is the absolute temperature, R is the gas constant, and ξ is a reduced density defined as

$$\xi = \frac{b}{4v} \quad (B.2)$$

parameter b reflects the hard-core size of the molecule and parameter a reflects the strength of attractive forces. Both parameters depend on temperature:

$$a = \alpha + \frac{\beta}{T} \quad (B.3)$$

Table B.1
Pure component parameters.

Component	c ($l\,mol^{-1}$)	a ($atm\,l^2\,mol^{-2}$)	β ($atm\,l^2\,mol^{-2}\,K$)	γ	δ ($\times 10^4\,K^{-1}$)
NH_3	0.01	2.6435	561.63	1.3884	1.470
CO_2	0.00	3.1693	253.17	1.2340	0.467
H_2O	0.01	3.1307	1161.63	1.5589	0.593

$$\log b = -\gamma - \delta T \tag{B.4}$$

where α, β, γ and δ are empirical constants. Also c is the characteristic constant. All constants and parameters of the pure components are given in Table B.1.

The fugacity coefficient is defined as:

$$\ln \phi_k = \left\{\frac{4\xi - 3\xi^2}{(1-\xi)^2}\right\} + \left(\frac{b_k}{b_M}\right)\left\{\frac{4\xi - 2\xi^2}{(1-\xi)^3}\right\} - \frac{2}{RTv}\left\{\sum_{j=1}^{m} y_i a_{kj}\right\} \times \left\{\sum_{n=1}^{5}\frac{(-1)^n}{n+1}\left(\frac{c_M}{v}\right)^n + 1\right\} + \frac{a_M c_k}{RTv^2}\left\{\sum_{n=1}^{4}\frac{(-1)^n(n+1)}{n+2}\left(\frac{c_M}{v}\right)^n + \frac{1}{2}\right\} - \ln z \tag{B.5}$$

Appendix C. Nomenclature

A_j jth parameter in the correlation of pure liquid reference fugacity of ammonia with temperature
a characteristic constant in equation state ($Pa\,m^6\,mol^{-2}$)
B_j jth parameter in the correlation of Henry's constant of carbon dioxide in water with temperature
b characteristic constant in equation state ($Pa\,m^6\,mol^{-2}\,K$)
C_i concentration of component i ($mol\,m^{-3}$)
c characteristic constant in equation state ($m^3\,mol^{-1}$)
E activation energy ($J\,mol^{-1}$)
$E_{c,j}$ residual function for chemical equilibrium relation for carbamate on the jth tray
$E_{i,j}$ residual function for phase equilibrium relation for component i on the jth tray
f_i fugacity of component i (kPa)
F matrix of functions
H_i liquid holdup on stage j (m^3)
$H^v_{i,j}$ enthalpy of component i in vapor phase on stage j ($J\,mol^{-1}$)
$H^l_{i,j}$ enthalpy of component i in liquid phase on stage j ($J\,mol^{-1}$)
ΔH heat of reaction ($J\,mol^{-1}$)
H_j residual function for total heat balance on the jth tray
H_{CO_2} Henry's constant of component i in solvent j
I ionic power in Table A.1
$K_{i,j}$ the equilibrium constant
k_0 pre-exponential factor of urea hydrolysis rate constant ($m^3\,mol^{-1}\,s^{-1}$)
k_f the forward reaction rate constant ($m^3\,mol^{-1}\,s^{-1}$)
$K_{x,r}$ equilibrium constant of reaction r dependent on temperature and mole fraction
$K_{\gamma,r}$ equilibrium constant of reaction r dependent on mole fraction
K_r equilibrium constant of reaction r dependent on temperature
l_i parameter of UNIQUAC equation in Table A.1
M number of components
$M_{i,j}$ residual function for material balance for component i on the jth tray
m_i molality of the ionic species i referred to 1000 g of mixed solvent ($kg\,(kg\,soln)^{-1}$)
N number of stages
P_j pressure of stage j (kPa)
ΔP_j pressure drop (kPa)
P_{top} pressure at the top of the urea thermal hydrolyser (kPa)
q_i UNIQUAC surface parameter of component i
r_i UNIQUAC volume parameter of component i
R universal gas constant ($J\,mol^{-1}\,K^{-1}$)
R^{ov}_j overall rate of reaction (1) on the jth tray ($mol\,m^{-3}\,s^{-1}$)
S^x_j residual function for summation relation in liquid phase on the jth tray
S^y_j residual function for summation relation in liquid phase on the jth tray
T temperature (K)
U constant (Eq. (12))
v^l_i liquid molal volume of component i
v^∞_i liquid molal volume of component i at infinite dilution
w consumption molar flow rate of carbamate in reaction (3) ($mol\,s^{-1}$)
$x_{i,j}$ mole fraction of component i in liquid phase on the jth tray
X matrix of output variables
$y_{i,j}$ mole fraction of component i in vapor phase on the jth tray
Z UNIQUAC coordination number ($Z = 10$) in Table A.1

Greek letters
$\alpha_{i,2}$ stoichiometric coefficient of species i in reaction (2)
$\alpha_{i,3}$ stoichiometric coefficient of species i in reaction (3)
a_{ij} parameter of UNIQUAC equation ($kJ\,mol^{-1}$) in Table A.1
γ_i activity coefficient of component i in Table A.1
$\bar{v}_i$ surface area fraction of component i in Table A.1
Φ_i volume area fraction of component i in Table A.1
τ_{ij} parameter of UNIQUAC equation in Table A.1
ξ reduced density in equation state

Subscripts
i component number
j stage number
r reaction number

Superscripts
C combinatorial
DH Debye–Huckel
RE residual
ov overall reaction

References

[1] M.A. Isla, H.A. Irazoqui, C.M. Genoud, Simulation of a urea synthesis reactor. Part 1. Thermodynamic framework, Ind. Eng. Chem. Res. 32 (1993) 2662–2670.
[2] V. Lagana, Process for Ammonia Production through Urea Hydrolysis, US Patent No. 5,399,755 (1995).
[3] N.J. Landis, Urea Hydrolysis, US Patent No. 4,341,640 (1982).
[4] J. Mehnen, C. Verweel, Experience to date with the Stamicarbon desorber–hydrolyser system, in: Proceedings of Stamicarbon's Seventh Urea Symposium, Maastrikht, The Netherlands, Paper 9, 1987, pp. 1–15.
[5] H. van Baal, The environmental impact of a Stamicarbon 2000 mtd urea plant, in: Proceedings of Eighth Stamicarbon Urea Symposium, Amsterdam, The Netherlands, 1996, pp. 4–7.
[6] Khorasan Petrochemical Company, Urea Plant, Operating Data of Urea Thermal Hydrolysis Process, 2008.
[7] M.R. Rahimpour, A. Azarpour, Simulation of a urea thermal hydrolysis reactor, Chem. Eng. Commun. 192 (2005) 155–167.

[8] M.R. Rahimpour, A non-ideal rate-based model for industrial urea thermal hydrolyser, Chem. Eng. Process. 43 (2004) 1299–1307.
[9] A.M. Douwes, Process for the Recovery of Valuable Components from the Waste Streams Obtained in the Preparation of Urea, US Patent No. 4,652,678 (1987).
[10] M. Brouwer, Has emission abatement a pay back time, in: Proceeding of Ninth Stamicarbon Urea Symposium, The Netherlands, 2000, pp. 6–16.
[11] I. Kroschwitz, M. Howe-Grant, Kirk-Othmer Encyclopedia of Chemical Technology, Suppl., fourth ed., Wiley, New York, 1995, pp. 597–621.
[12] M.R Rahimpour, A. Azarpour, A multistage well-mixed model for urea removal from industrial wastewater, Eng. Life Sci. 3 (2003) 335–340.
[13] M.M. Barmaki, M.R. Rahimpour, A. Jahanmiri, Treatment of wastewater polluted with urea by counter-current thermal hydrolysis in an industrial urea plant, Sep. Purif. Technol. 66 (2009) 492–503.
[14] M.R. Rahimpour, H.R. Mottaghi, M.M. Barmaki, Enhancement of urea, ammonia and carbon dioxide removal from industrial wastewater using a cascade of hydrolyser–desorber loops, Chem. Eng. J. 160 (2010) 594–606.
[15] Shiraz Petrochemical Complex, Urea Plant, Operating Data of Urea Thermal Hydrolysis Process, 2008.
[16] B. Claudel, E. Brousse, G. Shehadeh, Novel thermodynamic and kinetic investigation of ammonium carbamate decomposition into urea, Thermochim. Acta 102 (1986) 357–371.
[17] M. Boudart, Kinetics of Chemical Processes, Prentice-Hall, New Jersey, 1968.
[18] H. Eyring, E.M. Eyring, Modern Chemical Kinetics, Reinhold, New York, 1963.
[19] J.B. Butt, Reaction Kinetics and Reactor Design, second ed., Marcel Dekker, New York, 2000.
[20] R.J. Madon, E. Iglesia, Catalytic reaction rates in thermodynamically non-ideal systems, J. Mol. Catal. A: Chem. 163 (2000) 189–204.
[21] H. Aoki, T. Fujiwara, Y. Morozumi, T. Miura, Proceedings of the Fifth International Conference on Technologies and Combustion for a Clean Environment, Lisbon, 1999, pp. 115–118.
[22] T.F. Anderson, D.S. Abrams, E.A. Grens, Evaluation of parameters for nonlinear thermodynamics models, AICHE J. 24 (1978) 20–29.
[23] R. Nakamura, G.J.F. Breedveld, J.M. Prausnitz, Thermodynamic properties of gas mixtures containing common polar and nonpolar components, Ind. Eng. Chem. Process Des. Dev. 15 (1976) 557–564.
[24] A.L. Myers, W.D. Seider, Introduction to Chemical Engineering and Computer Calculation, Prentice-Hall, 1976.
[25] J.R. Friday, B.D. Smith, An analysis of the equilibrium stage separation problem formulation and convergence, AIChE J. 10 (1964) 698–707.
[26] J.D. Seader, E.J. Henley, Separation Process Principles, Wiley, New York, 1998.
[27] X. Zhang, S. Zhang, P. Yao, Y. Yuan, Modeling and simulation of high-pressure urea synthesis loop, Comput. Chem. Eng. 29 (2005) 983–992.
[28] M. Bernardis, G. Carvoli, M. Santini, Urea–NH_3–CO_2–H_2O: VLE calculations using an extended UNIQUAC equation, Fluid Phase Equilib. 53 (1989) 207–218.
[29] T.J. Edwards, G. Maurer, J. Newman, J.M. Prausnitz, Vapor–liquid equilibria in multicomponent aqueous solutions of volatile weak electrolytes, AIChE J. 24 (1978) 966–976.
[30] E.A. Kotula, A VLE model of the NH_3–CO_2–H_2O–urea system at elevated pressure, J. Chem. Technol. Biotechnol. 31 (1981) 103–110.
[31] M.A. Satyro, Y.K. Li, R.K. Agarwal, O.J. Santollani, Modeling Urea Processes: A New Thermodynamic Model and Software Integration Paradigm, 2001, http://www.cheresources.com.
[32] B. Sander, A. Fredenslund, P. Rasmussen, Calculation of vapour–liquid equilibria in mixed solvent/salt systems using an extended UNIQUAC equation, Chem. Eng. Sci. 41 (1986) 1171–1183.
[33] B. Sander, P. Rasmussen, A. Fredenslund, Calculation of vapor–liquid equilibrium in nitric acid–water–nitrate salt systems using an extended UNIQUAC equation, Chem. Eng. Sci. 41 (1986) 1185–1195.
[34] B. Sander, P. Rasmussen, A. Fredenslund, Calculation of solid–liquid equilibria in aqueous solutions of nitrate salts using an extended UNIQUAC equation, Chem. Eng. Sci. 41 (1986) 1197–1202.